Scientific Research Publishing

Optics and Photonics Journal, 2023, 13, 156-166
https://www.scirp.org/journal/opj
ISSN Online: 2160-889X
ISSN Print: 2160-8881

Synthesis of CC/$BiPO_4$/Bi_2WO_6 Composite Material and Its Photocatalytic Performance

Xiangdong Shi[1], Chaoyang Gao[2], Xiangyu Wei[2], Qingtao Chen[2], Fenghua Chen[2*], Guixia Liu[1*]

[1]School of Chemistry and Environmental Engineering, Changchun University of Science and Technology, Changchun, China
[2]School of Materials and Chemical Engineering, Zhengzhou University of Light Industry, Zhengzhou, China
Email: *liuguixia22@163.com, *phenix@ zzuli.edu.cn

How to cite this paper: Shi, X.D., Gao, C.Y., Wei, X.Y., Chen, Q.T., Chen, F.H. and Liu, G.X. (2023) Synthesis of CC/$BiPO_4$/Bi_2WO_6 Composite Material and Its Photocatalytic Performance. *Optics and Photonics Journal*, **13**, 156-166.
https://doi.org/10.4236/opj.2023.136014

Received: June 8, 2023
Accepted: June 27, 2023
Published: June 30, 2023

Abstract

Along with the popularity of environmental protection concepts, the environmental treatment of water pollution attracts widespread attention, among which, the research on Bi-based semiconductor photocatalytic degradation technology has made great progress. However, the development of such bismuth-based composites still remains a challenging task due to difficult recovery and low catalytic efficiency. Herein, a novel CC/$BiPO_4$/Bi_2WO_6 composite was successfully synthesized through two-step hydrothermal method using activated flexible carbon cloth as a substrate. The results of the photocatalytic degradation experiments showed that the obtained CC/$BiPO_4$/Bi_2WO_6 composites can degrade 92.1% RhB in 60 min under UV-visible light irradiation, which was much higher than that of unloaded $BiPO_4$ (24.4%) and $BiPO_4$/Bi_2WO_6 (52.9%), exhibiting a better adsorption-photocatalytic degradation performance than $BiPO_4$ and $BiPO_4$/Bi_2WO_6. Photoluminescence spectra indicated that the improved photocatalytic activity was due to the more effective inhibition of photogenerated carrier complexation. Furthermore, the radical capture experiments confirmed that h^+, ·OH and $\cdot O_2^-$ were the main active substances in the photocatalytic degradation process of RhB by the CC/$BiPO_4$/Bi_2WO_6 composites. More importantly, the prepared CC/$BiPO_4$/Bi_2WO_6 composite had a simple separation process and good recycling stability, and its photocatalytic degradation efficiency can still reach 53.3% after six cycles of RhB degradation.

Keywords

$BiPO_4$, Bi_2WO_6, Activated Flexible Carbon Cloth, Photocatalytic Degradation

1. Introduction

Environmental pollution, especially water pollution, caused by rapid industriali-

zation and population growth, poses a serious threat to human civilization [1]. Water is an important resource on which all living beings depend; however, domestic sewage, industrial and agricultural wastewater and other water bodies contain a large number of organic pollutants that are difficult to degrade and will cause a series of environmental pollution problems and damage ecosystems if discharged directly or indirectly without purification and treatment [2]. Therefore, the efficient removal of pollutants from the polluted water has attracted extensive attention from researchers [3]. The most promising approach to solve this problem in various wastewater treatment methods is semiconductor photocatalysis, and the preparation of environmentally efficient photocatalysts is the key to this photocatalytic technology [4].

In recent years, bismuth-based semiconductor photocatalysts have received much attention in the field of photocatalysis because of their unique electronic structure and photoelectric properties [5]. Among them, $BiPO_4$ is favored by researchers due to its good stability and high catalytic activity. However, its application is limited by the shortage of its photoresponse range limited to the UV region and high compounding rate of photogenerated carriers [6]. It has been reported in the literature that the photocatalytic activity can be improved by compounding with visible-light type Bi_2WO_6 semiconductor that can extend the light absorption range and promote the rapid separation of photogenerated charges [7] [8]. In addition, the preparation of photocatalysts loaded on activated flexible carbon cloth (CC) can not only improve adsorption capacity, increase the contact area between catalysts and pollutants, but also solve the problem of difficult separation of powder catalysts [9]. CC has high corrosion resistance, large specific surface area, excellent electrical conductivity and light transmission, and good stability and easy separation properties, which makes it a good loading material for adsorption and photocatalyst [10].

Therefore, in this paper, activated flexible carbon cloth (CC) was used as the substrate, and $BiPO_4$ and Bi_2WO_6 were sequentially loaded on the carbon cloth by hydrothermal method to finally obtain CC/$BiPO_4$/Bi_2WO_6 composite photocatalytic material, and the specific preparation process was shown in **Figure 1**.

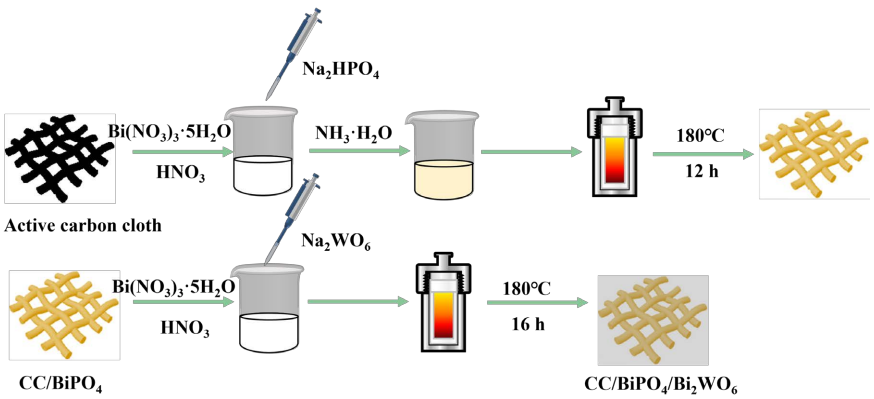

Figure 1. Experimental flowchart of the preparation of CC/$BiPO_4$/Bi_2WO_6 composite.

2. Experimental

2.1. Reagents

Bismuth nitrate pentahydrate ($Bi(NO)_3 \cdot 5H_2O$), disodium hydrogen phosphate dodecahydrate ($Na_2HPO_4 \cdot 12H_2O$), sodium tungstate dihydrate ($Na_2WO_6 \cdot 2H_2O$), ammonia, isopropyl alcohol, glacial acetic acid are all analytically pure and purchased from Sinopharm Chemical Reagent Co., Ltd.

2.2. Materials Preparation

Activation of carbon cloth: The 1 cm × 1 cm carbon cloth was placed in acetone, ethanol and water, respectively, and ultrasonically cleaned for 20 min. After cleaning, it was immersed in a mixed acid solution containing 30 mL of concentrated sulfuric acid and concentrated nitric acid 1:3 for 24 h. After completion, the carbon cloth was removed with tweezers, washed to neutral, and dried.

Preparation of CC/$BiPO_4$ composite: The treated carbon was arranged in 18 mL of 0.3 mol/L Bi $(NO)_3 \cdot 5H_2O$ solution containing 2 mL of concentrated nitric acid, and 15 mL of 0.3 mol/L $Na_2HPO_4 \cdot 12H_2O$ solution was added dropwise to it under magnetic stirring, and the pH was adjusted to 7 with ammonia, and then it was put into a reaction kettle at 180˚C for reaction for 12 h. After the reaction was completed, the carbon cloth was rinsed with water and ethanol, respectively, and dried at 60˚C. And the solution in the reaction kettle was washed by centrifugation to recover $BiPO_4$ powder and dried for use.

Preparation of CC/$BiPO_4$/Bi_2WO_6 composite: The prepared CC/$BiPO_4$ composite was immersed in 18 mL of 2 mol/L Bi $(NO)_3 \cdot 5H_2O$ solution containing 6 mL of glacial acetic acid for 12 h. Subsequently, 15 mL of 1 mol/L $Na_2WO_6 \cdot 2H_2O$ solution was added drop by drop, and finally the solution was loaded into a reaction kettle at 180˚C for 16 h. After the reaction, the solution was washed by centrifugation and the solid powder was recovered, the carbon cloth was removed and rinsed for use.

2.3. Photocatalytic Degradation of CC/$BiPO_4$/Bi_2WO_6

The prepared CC/$BiPO_4$/Bi_2WO_6 composite was placed in 10 mg/L RhB solution (40 mL) and stirred for 40 min under light-proof conditions to reach adsorption equilibrium, after which the supernatant was extracted by centrifugation every 10 min under the irradiation of a 500 W xenon lamp, and the photocatalytic process was detected in real time with a UV-Vis spectrophotometer.

2.4. Characterization

The morphology of the samples was characterized using a scanning electron microscope (SEM JSM-6490LV) from JEOL, Japan, and the crystalline structure of the samples was tested using a RIGAKU D/max 2500 X-ray diffractometer with a test voltage of 40 KV, a current of 20 mA, and a scan rate of 2˚/min, using a Cu target Kα1 radiation line (λ = 0.15405 nm). XPS was tested using a Thermo ESCALAB 250Xi tester, USA, with monochromatic Al Ka (hv = 1486.6 eV),

power 150 W, 500 μm beam spot, and binding energy calibrated at C1s 284.8. The UV spectra were tested in a Hitachi U-3900H UV-Visible spectrometer, Japan.

3. Results and Discussion

3.1. Crystal Structure, Morphology and Composition

Figure 2(a) and **Figure 2(b)** showed the SEM images of CC/$BiPO_4$ and CC/$BiPO_4$/Bi_2WO_6 composites. As illustrated in **Figure 2(a)**, the $BiPO_4$ was a one-dimensional nanorod structure. After loading Bi_2WO_6, the composite had a distinct layered two-dimensional morphology (**Figure 2(b)**), which indicated that the prepared CC/$BiPO_4$/Bi_2WO_6 had a large specific surface area that can provide multiple photocatalytic active sites. The EDS mapping of CC/$BiPO_4$/Bi_2WO_6 (**Figure 2(c)**) displayed that the surface of the CC/$BiPO_4$/Bi_2WO_6 composite contained Bi, P, W, and O elements, indicating that $BiPO_4$ and Bi_2WO_6 were successfully loaded on the carbon cloth.

Figure 3 showed the XRD patterns of CC, CC/$BiPO_4$ and CC/$BiPO_4$/Bi_2WO_6. In **Figure 3(a)**, the diffraction peaks located at 25.5˚ and 43.6˚ attributed to the graphitized carbon of carbon cloth. **Figure 3(b)** displayed the characteristic diffraction peaks of $BiPO_4$ at 2θ = 19.0, 21.7, 29.1, 31.2, 34.4, 36.8, 46.3, 52.8, 56.7 (JCPDS: 80-0287), indicating that the carbon cloth was successfully loaded with $BiPO_4$. **Figure 3(c)** showed sharp diffraction peaks of Bi_2WO_6 at 28.3˚, 32.8˚,

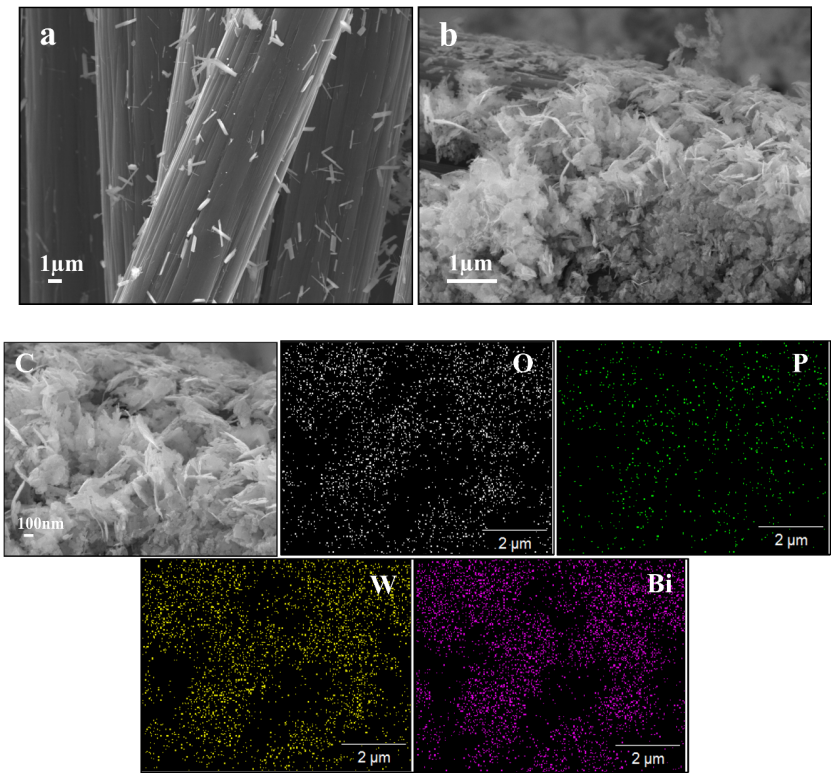

Figure 2. SEM images of the prepared CC/$BiPO_4$ (a) and CC/$BiPO_4$/Bi_2WO_6 (b); EDS mapping of CC/$BiPO_4$/Bi_2WO_6 (c).

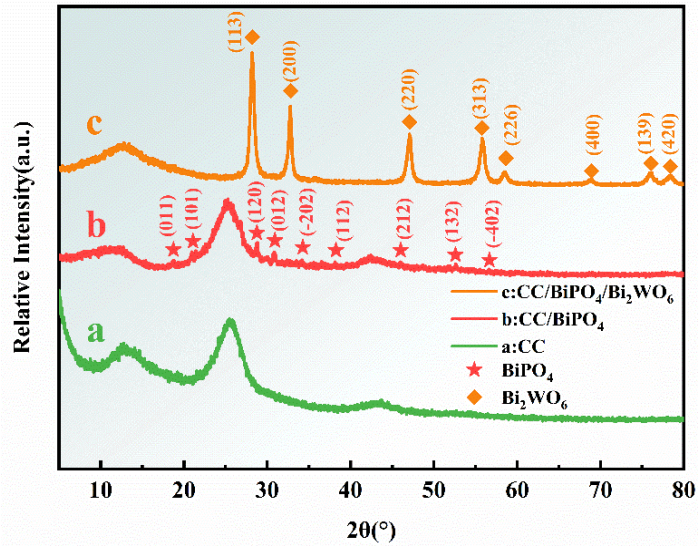

Figure 3. XRD patterns of the prepared CC, CC/$BiPO_4$ and CC/$BiPO_4$/Bi_2WO_6 photocatalyst.

47.2˚, 55.8˚, 58.6˚, 68.8˚, 75.9˚ and 78.4˚, corresponding to the (113), (200), (220), (313), (226), (400), (139) and (420) crystallographic planes (JCPDS No. 73-1126), respectively, indicating that the CC/$BiPO_4$ composite was further successfully loaded with Bi_2WO_6.

The surface compositions and chemical state of the prepared CC/$BiPO_4$/Bi_2WO_6 were confirmed by XPS spectra, which was illustrated in **Figure 4**. The survey spectrum of CC/$BiPO_4$/Bi_2WO_6 in **Figure 4(a)** clearly identified the existence of Bi, C, W, P, O. In **Figure 4(b)**, two characteristic peaks with binding energies of 159.12 and 164.47 eV belonged to Bi $4f_{7/2}$ and Bi $4f_{5/2}$ components, defining the existence of Bi^{3+} in the CC/$BiPO_4$/Bi_2WO_6 composite. The high resolution XPS of W 4f with binding energies located at 35.34 eV and 37.47 eV attributed to W $4f_{7/2}$ and W $4f_{5/2}$, respectively (**Figure 4(c)**). The characteristic peak of P 2p in the composite (**Figure 4(d)**) was located at E_B = 133.51 eV and the XPS profile of C 1s (**Figure 4(e)**) showed two characteristic peaks with binding energies at 284.17 eV and 285.54 eV corresponding to the C-C and C = C characteristic peaks of carbon cloth and the characteristic peak of activated carbon cloth, respectively.

3.2. UV Diffuse Reflectance Spectra

The UV diffuse reflectance spectra of CC, CC/$BiPO_4$ and CC/$BiPO_4$/Bi_2WO_6 as well as pure $BiPO_4$ and Bi_2WO_6 catalysts were shown in **Figure 5**. The absorption band edge of pure $BiPO_4$ is about 300 nm due to its large band gap energy (**Figure 5(d)**), while the optical response of the pure Bi_2WO_6 powder (**Figure 5(e)**) catalyst extended from the UV region to the visible region with band edge of 450 nm. After the powder sample was loaded on carbon cloth, the composite photocatalyst had absorption in the whole UV-visible region (200 - 800 nm) and enhanced the absorption intensity of visible light, which was more favorable for photocatalytic degradation of pollutants.

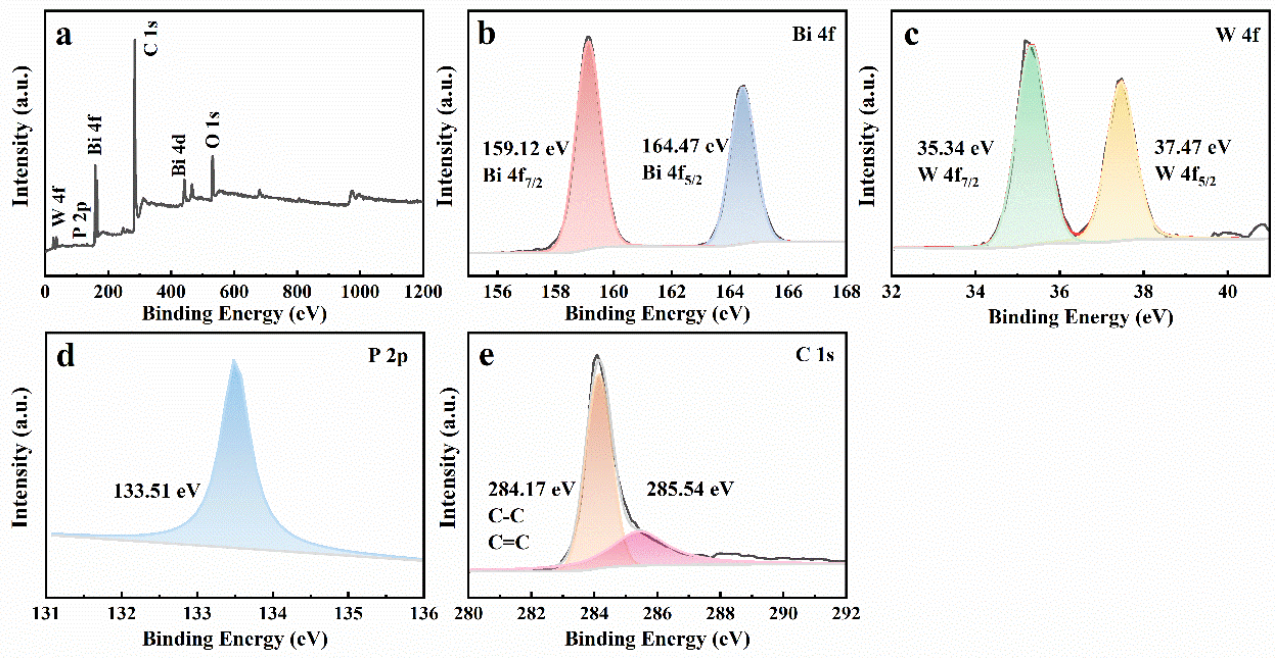

Figure 4. Survey XPS spectrum (a) and the high-resolution Bi 4f (b), W 4f (c), P 2p (d), and C1s (e) peaks of the prepared CC/$BiPO_4$/Bi_2WO_6 samples.

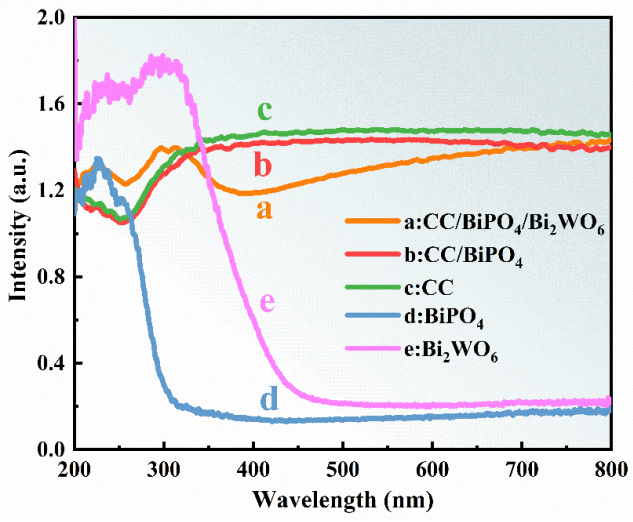

Figure 5. UV-vis diffuse reflection spectra of the prepared CC (a), CC/$BiPO_4$ (b), CC/$BiPO_4$/Bi_2WO_6 (c), $BiPO_4$ (d) and Bi_2WO_6 (e) samples.

3.3. Photocatalytic Performance

The photocatalytic degradation performance of the materials was investigated using $BiPO_4$, $BiPO_4$/Bi_2WO_6 and CC/$BiPO_4$/Bi_2WO_6 as catalysts, respectively, and the results were shown in **Figure 6**. **Figure 6(a)** displayed that adsorption equilibrium was reached at 40 min of stirring under the dark, at which the adsorption amounts of RhB molecules by $BiPO_4$, $BiPO_4$/Bi_2WO_6 and CC/$BiPO_4$/Bi_2WO_6 were 10.9%, 19.2% and 62.9%, respectively, and it can be concluded that the specific surface adsorption of RhB molecules by the composites increased

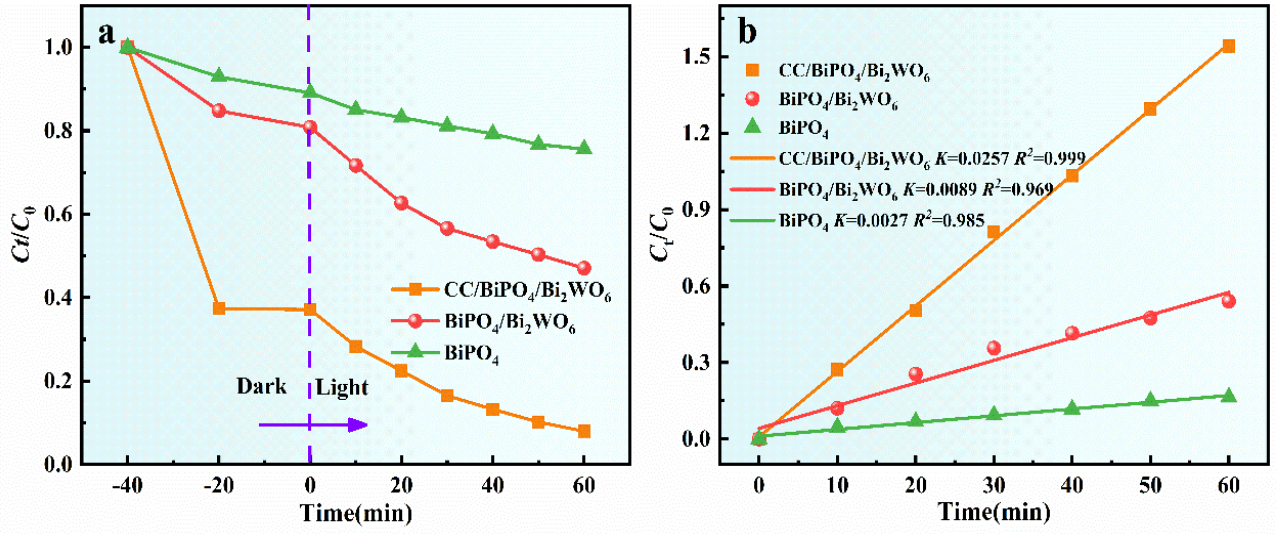

Figure 6. (a) Variations of RhB concentration as a function of irradiation time (with the time of light on set as 0) using $BiPO_4$, $BiPO_4/Bi_2WO_6$ and $CC/BiPO_4/Bi_2WO_6$ as photocatalysts. C_t is the RhB concentration at time t, and C_0 that in the initial solution. (b) Plots of ln (C_t/C_0) versus reaction time using $BiPO_4$, $BiPO_4/Bi_2WO_6$ and $CC/BiPO_4/Bi_2WO_6$ as photocatalysts.

after loading the sheet layer Bi_2WO_6. The removal rate of RhB by $CC/BiPO_4/Bi_2WO_6$ composite after UV-vis irradiation for 60 min was 92.1%, which was significantly higher than $BiPO_4$ (24.4%) and $BiPO_4/Bi_2WO_6$ (52.9%), and the removal effect originated from both of adsorption and catalytic degradation of RhB by $CC/BiPO_4/Bi_2WO_6$ composite. The absorption peak intensity of RhB in the UV spectrum was proportional to its concentration [11], so the reaction rate constant k was derived by fitting the reactant concentration as a function of time, and the results were shown in **Figure 6(b)**. **Figure 6(b)** showed that the reactions of photocatalytic degradation over RhB by $BiPO_4$, $BiPO_4/Bi_2WO_6$ and $CC/BiPO_4/Bi_2WO_6$ were all consistent with the first-order kinetic, and the reaction rate constants k for $CC/BiPO_4/Bi_2WO_6$ were 0.0257 min^{-1}, which was 9.5 and 2.9 times that of $BiPO_4$ (k = 0.0089 min^{-1}) and $BiPO_4/Bi_2WO_6$ (k = 0.0027 min^{-1}), respectively.

3.4. Photoluminescence Spectrum

The emission intensity of photoluminescence (PL) spectrum reflects the compounding efficiency of photoelectron-hole pairs, and the lower the emission intensity of PL spectrum, the lower the compounding rate of photogenerated e^- and h^+, and the higher the photocatalytic activity of the photocatalyst [12] [13]. **Figure 7** showed the PL spectra of $BiPO_4$, $BiPO_4/Bi_2WO_6$ and $CC/BiPO_4/Bi_2WO_6$ photocatalysts (λ_{ex} = 350 nm), from which it can be seen that the $CC/BiPO_4/Bi_2WO_6$ composite had the weakest luminescence peak intensity, indicating that loading the powdered $BiPO_4/Bi_2WO_6$ composite photocatalyst on carbon cloth can accelerate the photogenerated carrier mobility, slow down the compounding of photogenerated electron-hole pairs, and further improve the photocatalytic activity.

3.5. Radical Capture Experiments

To investigate the major active species of CC/$BiPO_4$/Bi_2WO_6 composites in the photocatalytic degradation of RhB by radical capture experiments [14], EDTA-2Na, p-benzoquinone (BQ) and isopropyl alcohol (IPA) were used as radical sacrificial agents for h^+, $\cdot O_2^-$ and ·OH, respectively. As can be seen from **Figure 8**, the catalytic activity of the CC/$BiPO_4$/Bi_2WO_6 catalyst was significantly reduced after the introduction of IPA, BQ and EDTA-2Na compared to the blank control without sacrificial agent, indicating that h^+, $\cdot O_2^-$ and ·OH were the main active species in the degradation process of RhB.

3.6. Cycle Stability Performance Test

The recyclability stability of photocatalysts plays a significant role in the practical application of photocatalysts [15]. When the photocatalytic reaction is finished, the prepared cloth-like CC/$BiPO_4$/Bi_2WO_6 composite can be easily removed from the solution with tweezers and rinsed several times with ultrapure water for the next catalytic degradation experiment. As shown in **Figure 9**, after

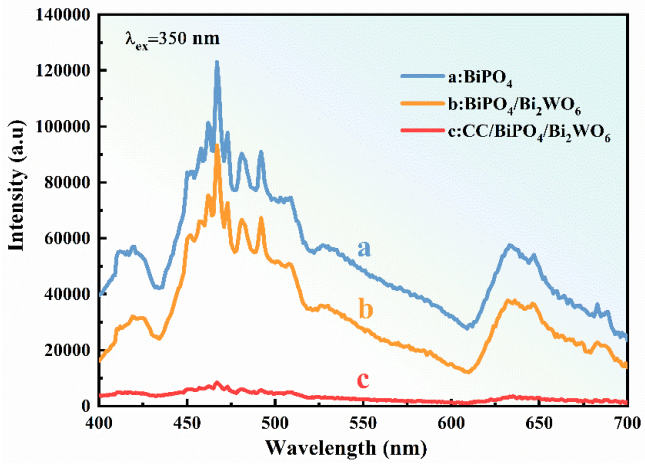

Figure 7. PL spectra of $BiPO_4$, $BiPO_4$/Bi_2WO_6 and CC/$BiPO_4$/Bi_2WO_6 photocatalysts (λex = 350 nm).

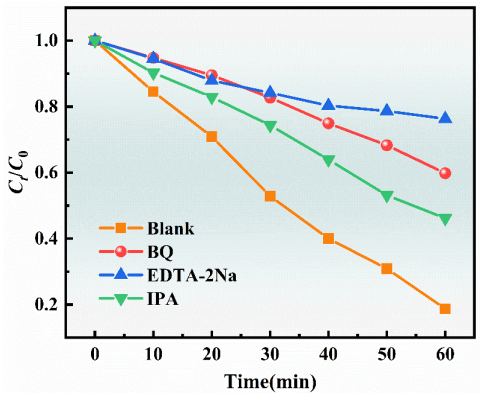

Figure 8. Photodegradation of RhB over the prepared CC/$BiPO_4$/Bi_2WO_6 photocatalyst in the presence of different scavengers (1 mL, 4 mM).

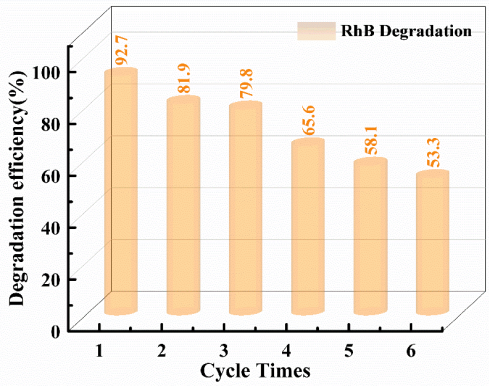

Figure 9. Relationship between the photocatalytic degradation efficiency of the prepared CC/$BiPO_4$/Bi_2WO_6 photocatalyst and cycle times.

the catalyst was recycled six times, the photocatalytic degradation efficiency was still up to 53.3% due to the shedding of a small amount of $BiPO_4$ and Bi_2WO_6, which had a certain stability of recycling, and CC/$BiPO_4$/Bi_2WO_6 composite reduced tedious steps such as centrifugal washing and recovery, compared to powder materials.

4. Conclusion

In this paper, CC/$BiPO_4$/Bi_2WO_6 composite was successfully synthesized through two-step hydrothermal method. The results of photocatalytic degradation experiments showed that CC/$BiPO_4$/Bi_2WO_6 had better adsorption-photocatalytic degradation performance than $BiPO_4$ and $BiPO_4$/Bi_2WO_6, and the removal rate of RhB by UV-visible light irradiation for 60 min was 92.1%, which was much higher than the powder unloaded $BiPO_4$ (24.4%) and $BiPO_4$/Bi_2WO_6 (52.9%). Photoluminescence spectra indicated that the improved photocatalytic activity was due to the more effective inhibition of photogenerated carrier complexes. Furthermore, the radical trapping experiments showed that h^+, $\cdot O_2^-$ and ·OH were the main active species in the photocatalytic degradation process of RhB. More importantly, CC/$BiPO_4$/Bi_2WO_6 composites had a simple separation process and good recycling stability, and the photocatalytic degradation efficiency can still reach 53.3% after six cycles.

Acknowledgements

This work was supported financially by the Science and Technology Development Project of Jilin Province (20220203170SF).

Conflicts of Interest

The authors declare no conflicts of interest regarding the publication of this paper.

References

[1] Bibi, S., Ahmad, A., Anjum, M.A.R., Haleem, A., Siddiq, M. and Shah, S.S. (2021)

Photocatalytic Degradation of Malachite Green and Methylene Blue over Reduced Graphene Oxide (rGO) Based Metal Oxides (rGO-Fe_3O_4/TiO_2) Nanocomposite under UV-Visible Light Irradiation. *Journal of Environmental Chemical Engineering*, ***9***, Article ID: 105580. https://doi.org/10.1016/j.jece.2021.105580

[2] Hunge, Y.M., Yadav, A.A., Khan, S., Takagi, K., Suzuki, N. and Teshima, K. (2021) Photocatalytic Degradation of Bisphenol A Using Titanium Diox ide@nanodiamond Composites under UV Light Illumination. *Journal of Colloid and Interface Science*, **582**, 1058-1066. https://doi.org/10.1016/j.jcis.2020.08.102

[3] Tang, Y.D., Li, T., Xiao, W.X., Huang, Z.T., Wen, H.C., Situ, W. and Song, X.L. (2023) Degradation Mechanism and Pathway of Tetracycline in Milk by Heterojunction N-TiO_2-Bi_2WO_6 Film under Visible Light. *Food Chemistry*, **401**, Article ID: 134082. https://doi.org/10.1016/j.foodchem.2022.134082

[4] Zhang, B., He, X., Yu, C.Z., Liu, G.C., Ma, D., Cui, C.Y., Yan, Q.H., Zhang, Y.J., Zhang, G.S. and Ma, J. (2022) Degradation of Tetracycline Hydrochloride by Ultrafine TiO_2 Nanoparticles Modified g-C_3N_4 Heterojunction Photocatalyst: Influencing Factors, Products and Mechanism Insight. *Chinese Chemical Letters*, **33**, 1337-1342. https://doi.org/10.1016/j.cclet.2021.08.008

[5] Liu, L., Liu, J., Sun, K., Wan, J., Fu, F. and Fan, J. (2021) Novel Phosphorus-Doped Bi_2WO_6 Monolayer with Oxygen Vacancies for Superior Photo Catalytic Water Detoxication and Nitrogen Fixation Performance. *Chemical Engineering Journal*, **411**, Article ID: 128629. https://doi.org/10.1016/j.cej.2021.128629

[6] Tang, M., Li, X., Deng, F., Han, L., Xie, Y. and Huang J. (2023) $BiPO_4$/Ov-BiOBr High-Low Junctions for Efficient Visible Light Photocatalytic Performance for Tetracycline Degradation and H_2O_2 Production. *Catalysts*, **13**, 634. https://doi.org/10.3390/catal13030634

[7] Kumar, R., Raizada, P., Khan, A.A.P., Nguyen, V.H., Van, L.Q. and Ghotekar, S. (2022) Recent Progress in Emerging $BiPO_4$-Based Photocatalysts: Synthesis, Properties, Modification Strategies, and Photocatalytic Applications. *Journal of Materials Science & Technology*, **108**, 208-225. https://doi.org/10.1016/j.jmst.2021.08.053

[8] Zhu, Y., Wang, Y., Ling, Q. and Zhu, Y. (2017) Enhancement of Full-Spectrum Photocatalytic Activity over $BiPO_4$/Bi_2WO_6 Composites. *Applied Catalysis B*: *Environmental*, **200**, 222-229. https://doi.org/10.1016/j.apcatb.2016.07.002

[9] Shao, M., Feng, X., Liu, D. and Zhang, Y. (2023) A Layer by Layer Strategy for the TiO_2/Cu_xO/CeO_2 Hierarchical Structure Supported on Carbon Cloth as a Photocarrier-Assisted Photothermal Catalyst with Fast Visible Light Response. *Materials Chemistry Frontiers*, **7**, 745-752. http://dx.doi.org/10.1039/D2QM01189A

[10] Jiang, L.C., Gao, X.Y., Chen, S.L., Ashok, J. and Kawi, S. (2021) Oxygen-Deficient WO_3/TiO_2/CC Nanorod Arrays for Visible-Light Photocatalytic Degradation of Methylene Blue. *Catalysts*, **11**, 1349. https://doi.org/10.3390/catal11111349

[11] Wang, Y., Rao, L., Wang, P., Shi, Z. and Zhang, L. (2020) Photocatalytic Activity of N-TiO_2/O-Doped N Vacancy g-C_3N_4 and the Intermediates Toxicity Evaluation under Tetracycline Hydrochloride and Cr (VI) Coexistence Environment. *Applied Catalysis B*: *Environmental*, **262**, Article ID: 118308. https://doi.org/10.1016/j.apcatb.2019.118308

[12] Tang, T., Yin, Z.L., Chen, J.R., Zhang, S., Sheng, W.C., Wei, W.X., Xiao, Y.G., Shi Q.Y. and Cao, S.S. (2021) Novel p-n Heterojunction Bi_2O_3/Ti^{3+}-TiO_2 Photocatalyst Enables the Complete Removal of Tetracyclines under Visible Light. *Chemical Engineering Journal*, **417**, Article ID: 128058 https://doi.org/10.1016/j.cej.2020.128058

[13] Chen, F.H., Liang, W.W., Qin, X.Y., Jiang, L.Y., Zhang, Y.H., Fang, S.M. and Luo,

D. (2021) Ag@AgCl Photocatalyst Loaded on the 3D Graphene/PANI Hydrogel for the Enhanced Adsorption-Photocatalytic Degradation and *In Situ* SERS Monitoring Properties. *Chemistryselect*, **6**, 4166-4177. https://doi.org/10.1002/slct.202100580

[14] Ni, J.X., Wang, W., Liu, D.M., Zhu, Q., Jia, J.L., Tian J.Y., Li, Z.Y., Wang, X. and Xing, Z.P. (2021) Oxygen Vacancy-Mediated Sandwich-Structural TiO_{2-x}/Ultrathin g-C_3N_4/TiO_{2-x} Direct Z-Scheme Heterojunction Visible-Light-Driven Photocatalyst for Efficient Removal of High Toxic Tetracycline Antibiotics. *Journal of Hazardous Materials*, **408**, Article ID: 124432. https://doi.org/10.1016/j.jhazmat.2020.124432

[15] Hieu, V.Q., Phung, T.K., Nguyen, T.Q., Khan, A., Doan, V.D. and Tran, V.A. (2021) Photocatalytic Degradation of Methyl Orange Dye by Ti_3C_2-TiO_2 Heterojunction under Solar Light. *Chemosphere*, **276**, Article ID: 130154. https://doi.org/10.1016/j.chemosphere.2021.130154